

Injected Power Fluctuations in Langevin Equation

Jean Farago*

*Laboratoire de Physique Statistique, École Normale Supérieure[†]
24 rue Lhomond, 75231 Paris cedex 05, France.*

Abstract

Using path integral method, we compute exactly the probability density function of the power (averaged over a large time interval of length τ) injected (and dissipated) by the random force into a Brownian particle driven by a Langevin equation. The resulting distribution, as well as the associated large deviation function, display strong asymmetry, whose origin is discussed. Moreover, the so-called “Fluctuation Theorem” is shown not to be verified in this dissipative system, although any numerical or experimental evidence of this violation would be extremely difficult to establish. Finally, we show, using numerical simulations, that this distribution seems to be insensitive to the presence of a pinning potential, despite a large disparity of typical behaviours of the Brownian particle motions; this addresses the question of possible universality of the large deviation function of the injected power in the 1D Langevin context.

Keywords: Fluctuation phenomena, random processes, noise and Brownian motion.

1 Introduction

Usually, works concerning out of equilibrium stationary systems deal with their local statistical properties, some assumptions of homogeneity and isotropy being reasonably assumed or understood: traditional theory of turbulence, which focuses on local correlations of the velocity field furnishes a good archetype of that. A rather new way to study such systems was recently proposed by some authors [1, 2, 3], who preferred concentrate their efforts to characterize the process of injection of energy, imperatively required to sustain the stationary state. To be more precise, in numbers of such situations, there exists a channel of energy injection, usually located at boundaries of the system (rotating blades driving a turbulent flow, heated plate in Rayleigh-Bénard convection, piston shaking granular matter at an edge of a vessel, etc . . .) together with a distinct channel of dissipation, often provided by a bulk dissipation mechanism, viscosity or inelastic collisions. This duality is explicitly expressed in the dynamical equation for the energy which can always be written in the form $\dot{E} = I - D$, where D is proportional to a coefficient of dissipation whereas I is entirely due to the injection process. These two distinct “gates” lead to establishment of a permanent flow of energy throughout the system, and is obviously a primordial feature amongst the stationary properties of the system. Thus, some experimental measurements [1, 2, 3] and numerical

*e-mail: farago@lps.ens.fr

[†]CNRS, UMR 8550

simulations [4] were performed to characterize the injection of energy (more easily reachable than the dissipation), or more precisely the probability density function (pdf) $\pi_{inj}(\varepsilon)$ of the averaged injected power during a time interval of length τ (an averaging originally due to experimental limitations).

The initial aim of this paper is to provide a simple model, where the pdf π_{inj} is exactly computable, and which mimics as simply as possible the presence of two distinct channels for energy flow. One of the simplest (nontrivial) systems fulfilling these requirements is provided by the Langevin equation

$$\dot{v} + \gamma v = \psi(t) \quad (1)$$

$$\langle \psi(t)\psi(t') \rangle = 2\gamma k_B T \delta(t - t') \quad (2)$$

where fluctuations $\psi(t)$ and dissipation γv are considered as two different sources of modification of energy :

$$\frac{d}{dt} \left(\frac{1}{2} v^2 \right) = \underbrace{-\gamma v^2}_{\text{dissipation}} + \underbrace{\psi v}_{\text{injection}} \quad (3)$$

Note that in absence of ψ , the system is clearly dissipative and non time-reversal invariant, a property also shared by realistic hydrodynamic or granular systems.

We show in the following how to calculate the pdf of

$$\varepsilon = \frac{1}{\tau} \int_t^{t+\tau} dt' \psi(t') v(t') \quad (4)$$

using the path integral method (we compute also in appendix B the pdf of the dissipated power). We analyse in details the limit of large τ , and discuss some properties of π_{inj} in this limit : we will see that the so-called “Fluctuation Theorem” [5, 6] is not verified in that case, in agreement with arguments given in [4]. Some surprising features emerge also from our study, namely the fact that this pdf seems to be almost insensitive to the dynamical details of the model (if one modifies the Langevin equation by adding a potential, for instance), even when typical dynamical behaviours of the particle are extremely different from each other : this seemingly common limiting distribution, perhaps a consequence of the presence of a fluctuation-dissipation balance, suggests nevertheless the relevance of considering the averaged injected power as a probe for extracting global features of energy flow into a nonequilibrium system.

2 Free Brownian motion

2.1 System

The evolution of the free particle experiencing a Langevin white noise is given by (1) One wishes to compute the probability distribution function (pdf) of the variable

$$\varepsilon = \lim_{t \rightarrow \infty} \frac{1}{\tau} \int_t^{t+\tau} dt' \psi(t') v(t') \quad (5)$$

which is nothing but the mean power given to the Brownian particle by the thermostat during a time interval τ , at thermal equilibrium (the $t \rightarrow \infty$ limit guarantees the irrelevance of possible non-thermalized initial conditions).

It is more convenient to compute rather the Fourier transform of this pdf :

$$\hat{\pi}_{inj}(k) \equiv \left\langle \exp \frac{ik}{\tau} \lim_{t \rightarrow \infty} \int_t^{t+\tau} dt' \psi(t') v(t') \right\rangle \quad (6)$$

2.2 Limit $t \rightarrow \infty$

One can express the mean in terms of path integral as

$$\hat{\pi}_{inj} \propto \lim_{t \rightarrow \infty} \int \mathcal{D}\psi e^{-\frac{1}{4k_B T \gamma} \int dt' \psi^2(t')} \exp \left(\frac{ik}{\tau} \int_t^{t+\tau} dt' \psi(t') \int_0^{t'} du e^{-\gamma(t'-u)} \psi(u) \right) \quad (7)$$

The transform

$$\int_t^{t+\tau} dt' \psi(t') \int_0^{t'} du e^{-\gamma(t'-u)} \psi(u) = \int_{-\tau/2}^{\tau/2} dt' \psi(t'+t+\tau/2) \int_0^{t'+t+\tau/2} du e^{-\gamma u} \psi(t'+t+\tau/2-u) \quad (8)$$

combined with the time translational invariance of the noise followed by the $t \rightarrow \infty$ limit allows to recast $\hat{\pi}_{inj}$ in the form

$$\hat{\pi}_{inj} \propto \int \mathcal{D}\psi e^{-\frac{1}{4k_B T \gamma} \int dt' \psi^2(t')} \exp \left(\frac{ik}{\tau} \int dt_1 dt_2 \psi(t_1) \psi(t_2) g(t_1, t_2) \right) \quad (9)$$

with

$$g(t_1, t_2) = \chi_{[-\tau/2, \tau/2]}(t_1) \theta(t_1 - t_2) \exp(-\gamma(t_1 - t_2)) \quad (10)$$

(χ is the indicator function and θ the Heaviside function).

2.3 Separation $t \in [-\infty; -\tau/2]$ vs. $t \in [-\tau/2; \tau/2]$

One can split the mean in two (correlated) contributions :

$$\begin{aligned} \hat{\pi}_{inj} &\propto \int \mathcal{D}\psi e^{-\frac{1}{4k_B T \gamma} \int dt' \psi^2(t')} \underbrace{\exp \left(\frac{ik}{\tau} \int_{-\frac{\tau}{2}}^{\frac{\tau}{2}} dt_1 dt_2 \psi(t_1) \psi(t_2) g(t_1, t_2) \right)}_{\equiv W_+} \\ &\times \exp \left(\frac{ik}{\tau} \int_{-\frac{\tau}{2}}^{\frac{\tau}{2}} dt_1 \psi(t_1) e^{-\gamma t_1} \int_{-\infty}^{-\frac{\tau}{2}} dt_2 \psi(t_2) e^{\gamma t_2} \right) \end{aligned} \quad (11)$$

$$\begin{aligned} &\propto \int \mathcal{D}\psi_+ e^{W_+ - \frac{1}{4k_B T \gamma} \int_{-\frac{\tau}{2}}^{\frac{\tau}{2}} \psi_+^2} \\ &\times \underbrace{\int \mathcal{D}\psi_- \exp \left(-\frac{1}{4k_B T \gamma} \int_{-\infty}^{-\frac{\tau}{2}} \psi_-^2 + \frac{ik}{\tau} \int_{-\frac{\tau}{2}}^{\frac{\tau}{2}} dt_1 \psi_+(t_1) e^{-\gamma t_1} \int_{-\infty}^{-\frac{\tau}{2}} dt_2 \psi_-(t_2) e^{\gamma t_2} \right)}_{\equiv B} \end{aligned} \quad (12)$$

In these expressions, the indices $+/$ refer to the half paths corresponding to the time intervals $[-\tau/2; \tau/2]$ and $[-\infty; -\tau/2]$ respectively.

The piece B can be explicitly calculated, since the integral is Gaussian and unconstrained with respect to ψ_+ (the result will involve nevertheless ψ_+ , for it appears in the integrand). Let define $u = 2\gamma k_B T k / \tau \times \int_{-\tau/2}^{\tau/2} dt_1 \psi_+(t_1) e^{-\gamma t_1}$. One gets

$$B = \int \mathcal{D}\psi_- \exp \left[-\frac{1}{4k_B T \gamma} \int_{-\infty}^{-\tau/2} dt' \left(\psi_-(t') - iue^{\gamma t'} \right)^2 - \frac{u^2}{4k_B T \gamma} \int_{-\infty}^{-\tau/2} dt' e^{2\gamma t'} \right] \quad (13)$$

$$\propto \exp -\frac{e^{-\gamma\tau} k^2 k_B T}{2\tau^2} \left[\int dt' \psi_+(t') e^{-\gamma t'} \right]^2 \quad (14)$$

As the coefficient of proportionality is independent of k , the last expression is indeed the exact result for B , since $B = 1$ if $k = 0$.

One could ask why it is useful to perform such a partial integration, and whether it would be possible to diagonalize directly the operator g . The reason is that the diagonalization of g , though easily performed, gives a set of eigenfunctions which is far from being complete. The preliminary summation over ψ_- repairs this problem.

2.4 Diagonalization

One introduces the operator \mathcal{T} defined as :

$$(\mathcal{T}\phi)(t) \equiv \int_{-\tau/2}^{\tau/2} dt' \phi(t') e^{-\gamma|t-t'|} \quad (15)$$

The pdf thus reads

$$\hat{\pi}_{inj} \propto \int \mathcal{D}\psi_+ \exp \left(-\frac{1}{4k_B T \gamma} \int_{-\tau/2}^{\tau/2} \psi_+^2 + \frac{ik}{2\tau} \int_{-\tau/2}^{\tau/2} \psi_+ (\mathcal{T}\psi_+) - \frac{k^2 k_B T}{2\tau^2} [\mathcal{T}\psi_+(-\tau/2)]^2 \right) \quad (16)$$

Let assume that one can diagonalize this operator, that is one knows a set $(\phi_n, \xi_n)_{n \in \mathbb{N}^*}$ such that

$$\mathcal{T}\phi_n(t) = \xi_n \phi_n(t) \quad (17)$$

$$\int_{-\tau/2}^{\tau/2} \phi_n \phi_m = \delta_{n,m} \quad (18)$$

One will assume that this set is sufficient to sample the paths ψ_+ (one could probably verify that the Hilbert subspace of $L^2([-\tau/2, \tau/2])$ generated by the ϕ_n is dense, since it is formed by functions C^2 having peculiar boundary conditions at $\pm\tau/2$, cf. next section).

As a result,

$$\hat{\pi}_{inj} \propto \int d\mathbf{a} \exp \left(-\frac{1}{4k_B T \gamma} \sum_n a_n^2 + \frac{ik}{2\tau} \sum_n \xi_n a_n^2 - \frac{k^2 k_B T}{2\tau^2} \left[\sum_n a_n \xi_n \phi_n(-\tau/2) \right]^2 \right) \quad (19)$$

This expression is further simplified with the help of an auxiliary variable :

$$\hat{\pi}_{inj} \propto \int_{-\infty}^{\infty} dr e^{-r^2} \int da \exp \left(-\frac{1}{4k_B T \gamma} \sum_n a_n^2 + \frac{ik}{2\tau} \sum_n \xi_n a_n^2 + i \frac{\sqrt{2k_B T} kr}{\tau} \left[\sum_n a_n \xi_n \phi_n(-\frac{\tau}{2}) \right] \right) \quad (20)$$

$$\propto \int_{-\infty}^{\infty} dr e^{-r^2} \prod_n \int da_n \exp \left(-a_n^2 (1 - 2i\tilde{k}\xi_n) + 2ir\tilde{k}\sqrt{2\gamma}\xi_n \phi_n(-\frac{\tau}{2}) a_n \right) \quad (21)$$

$$= \exp \left(-\frac{1}{2} \sum_n \log(1 - 2i\tilde{k}\xi_n) - \frac{1}{2} \log \left(1 + 2\gamma\tilde{k}^2 \sum_n \frac{\xi_n^2 \phi_n(-\frac{\tau}{2})^2}{1 - 2i\tilde{k}\xi_n} \right) \right) \quad (22)$$

where

$$\tilde{k} \equiv k \times \frac{k_B T}{\tau} \quad (23)$$

stands for the dimensionless conjugate coordinate. Note that (22) is the exact formal result since $\hat{\pi}_{inj}(k=0) = 1$.

2.5 Determination of eigenvalues and eigenfunctions of \mathcal{T}

It is easy to verify that the eigenfunctions of \mathcal{T} obey an ordinary differential equation :

$$\underbrace{\phi_n'' + \frac{\gamma}{\xi_n} (2 - \gamma \xi_n) \phi_n}_\equiv = 0 \quad (24)$$

(obtained by differentiation of 17). The eigenmodes are then given by

$$\phi_n(t) = A_n e^{i\omega_n t} + B_n e^{-i\omega_n t} \quad (25)$$

(the frequencies ω_n being a priori real positive or purely imaginary). When this is substituted into the integral equation, one gets two linear equations

$$\frac{A_n}{\gamma + i\omega_n} e^{-i\omega_n \tau/2} + \frac{B_n}{\gamma - i\omega_n} e^{i\omega_n \tau/2} = 0 \quad (26)$$

$$\frac{A_n}{-\gamma + i\omega_n} e^{i\omega_n \tau/2} - \frac{B_n}{\gamma + i\omega_n} e^{-i\omega_n \tau/2} = 0 \quad (27)$$

whence one extracts the solvability condition for the eigenfrequencies :

$$e^{2i\omega_n \tau} = \left(\frac{\omega_n + i\gamma}{\omega_n - i\gamma} \right)^2 \quad (28)$$

In this equation, the right hand side is a complex whose argument is in $[-\pi/2, \pi/2]$ (one can verify that only $\omega_n \in \mathbb{R}^+$ is possible) ; this gives the implicit equation fulfilled by $x_n = \omega_n/\gamma$:

$$\tilde{\gamma} x_n + 2 \operatorname{Atan} x_n = n\pi \quad (29)$$

with $\tilde{\gamma} \equiv \gamma\tau$

As a result, one has simply $A_n/B_n = (-1)^{n+1}$. Thus, according as n is odd or even, ϕ_n is $\phi_n = \rho_n \cos \omega_n t$ or $\phi_n = \rho_n \sin \omega_n t$, with ρ_n given by the normalization condition. For instance, one has for even n :

$$1 = \int_{-\tau/2}^{\tau/2} dt \phi_n(t)^2 = \frac{\rho_n^2 \tau}{2} \left(\frac{\sin \omega_n \tau}{\omega_n \tau} + 1 \right) = \frac{\rho_n^2 \tau}{2} \left(\frac{2/\tilde{\gamma}}{1 + x_n^2} + 1 \right) \quad (30)$$

For odd n , this result is still valid. One has also to compute $\phi_n^2(-\tau/2)$; its expression,

$$\phi_n^2(-\tau/2) = \frac{2\omega_n^2/\tau}{2\gamma/\tau + \gamma^2 + \omega_n^2} \quad (31)$$

holds also whatever the parity of n .

One must pay attention to the fact that $n = 0$ ($\omega_0 = 0$) is not a valid eigenvalue, since it would imply $\phi_0 = 0$. This reflects the fact that the Hilbert space generated by the ϕ_n does not match entirely $L^2([-\tau/2, \tau/2])$, but is restricted to functions f twice differentiable, such that (cf. [7])

$$\frac{1}{2\gamma} \mathcal{T}[f'' - \gamma^2 f] = -f \quad (32)$$

$$\iff \begin{cases} f'(\frac{\tau}{2}) + \gamma f(\frac{\tau}{2}) = 0 \\ f'(-\frac{\tau}{2}) - \gamma f(-\frac{\tau}{2}) = 0 \end{cases} \quad (33)$$

We assume this subspace to be large enough to sample accurately the whole L^2 space (one has probably to require the subspace considered to be densely immersed in L^2 , what is easily proved, due to the local character of conditions (33)).

2.6 Structure of the pdf

Taking into account the computations of the previous section one has that

$$\begin{aligned} \hat{\pi}_{inj} = \exp \left(-\frac{1}{2} \sum_{n=1}^{\infty} \log \left(1 - \frac{4i\tilde{k}}{1+x_n^2} \right) \right. \\ \left. - \frac{1}{2} \log \left(1 + 16\tilde{k}^2 \sum_{n=1}^{\infty} \frac{x_n^2}{1+x_n^2} \frac{1}{2+\tilde{\gamma}(1+x_n^2)} \frac{1}{1-4i\tilde{k}+x_n^2} \right) \right) \end{aligned} \quad (34)$$

This function is analytical in a large part of the complex plane. The sole breakdown of analyticity arises from the cuts implicitly assumed in the use of the *log*. These logarithms come from Gaussian integration $\int dx \exp(-zx^2) = \sqrt{\pi/z} = \exp(\log(\pi/z)/2)$, so they have a cut along the negative real axis. In terms of the k variable, it leads to cuts along half vertical lines: first, $\hat{\pi}_{inj}$ has singularities whenever $1 - 4i\tilde{k}/(1+x_n^2) = 0$. It leads then *a priori* to a cut along the vertical negative axis, defined by $\tilde{k} \in i[-\infty, -1/4]$ (a more careful inspection shows that the analyticity is restored in the segments $i[-\tilde{k}_-^{(2n+2)}, -\tilde{k}_-^{(2n+1)}]$, where $\tilde{k}_-^{(p)} = (1+x_p^2)/4$; but this property is in fact of little importance in the following ...). But a second source of non-analyticity is provided by the “isolated” *log* in the exponential of (34): $\hat{\pi}_{inj}$ is not defined if the argument of this *log* is negative ; this is true in particular if $\tilde{k} \in i[\tilde{k}_+, \infty[$, with $\tilde{k}_+ > 0$ defined by

$$\frac{1}{16\tilde{k}_+^2} = \sum_n \frac{x_n^2}{1+x_n^2} \frac{1}{2+\tilde{\gamma}(1+x_n^2)} \frac{1}{1+4\tilde{k}_++x_n^2} \quad (35)$$

This second term gives also other small excluded segments located in the negative real axis, also caused by the poles $\tilde{k}_-^{(p)}$; they enlarge somewhat the segments already mentioned.

It would be interesting to provide a physical interpretation of these cuts, in a similar way one can interpret the poles and cuts of Laplace transforms of Green functions of a

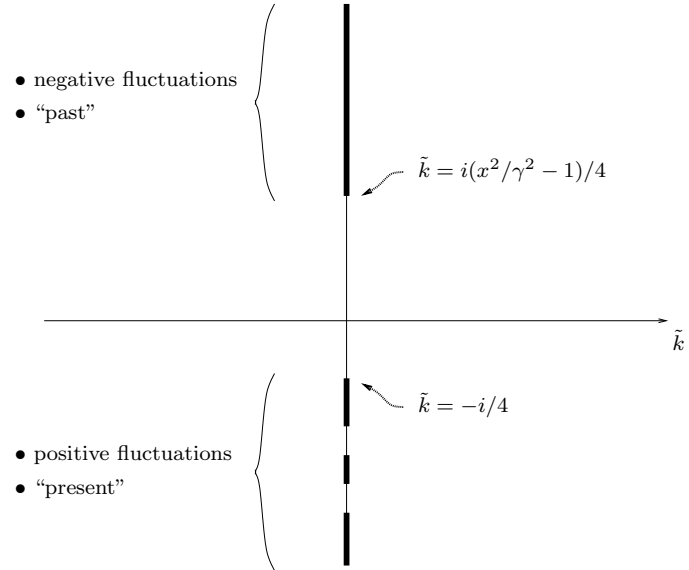


Figure 1: Sketch of the cuts in the \tilde{k} -plane. See details in the text.

linear system in terms of localized modes and phonons bands. However, such a physical identification is not as limpid here. The derivation of the result implies a separation of a contribution due to the “past” of the dynamics (the part B of the path integral), and another implying only the “present” of the dynamics (i.e. the period of power average). Consequently, one can assign the presence of the cut on the upper vertical axis to a contribution of the “past” of the particle, mediated through time-correlations of the process $v(t)$ (cf. fig 1). Conversely, the lower cut is related to the term $\int \psi \mathcal{T} \psi$, which implies only the knowledge of the present of the particle: all the excluded segments in $i\mathbb{R}^-$ can be assigned to ψ_- ; nevertheless, the physical interpretation of the “island” structure of this negative cut is at present not clear.

This discussion leads to an important conclusion concerning the pdf in the direct space: as this pdf is given by

$$\pi_{inj}(\varepsilon) = \int \frac{dk}{2\pi} \hat{\pi}_{inj}(k) e^{-ik\varepsilon}, \quad (36)$$

one sees that the path of integration can be deformed in a way depending on the sign of ε ; if ε is *positive*, one can stick the integration path on both sides of the *negative* (imaginary) cut, whereas if $\varepsilon < 0$, this deformation can be performed toward the upper cut.

As a result, the negative fluctuations in the injected power appear to be drastically related to the past history of the particle and to the presence of correlations in its velocity. This result is quite natural, since the appearance of negative fluctuations in the injected power comes from the inertia of the particle, which does not adjust itself instantaneously to receive thermal energy always efficiently.

2.7 Limit $\gamma\tau \gg 1$

The limit of large τ is interesting, since it corresponds more or less to experimental situations, where measurements are usually performed on time scales far larger than the dissipation time scale (here γ^{-1}). Moreover, the fluctuation theorem is established in this limit only, and it is interesting to check if this simple system verifies this theorem or not. We will see also that it leads to simple formulae, in comparison with (22) or (34).

The large τ -limit must be carefully performed, in order to keep all relevant terms for the leading asymptotics.

Let us compute the pdf of the dimensionless variable $\tilde{\varepsilon} = \varepsilon\tau/k_B T$

$$\pi(\tilde{\varepsilon}) = \int \frac{d\tilde{k}}{2\pi} e^{-i\tilde{k}\tilde{\varepsilon}} \hat{\pi}_{inj}(\tilde{k}) \quad (37)$$

This integral is of the form

$$I(\tau) = \int d\tilde{k} \exp[\tau\Phi(\tau, \tilde{k})] \quad (38)$$

with Φ of order τ^0 . What is the leading order of such an integral when $\tau \rightarrow \infty$? If one assumes the following expansion of Φ for large τ ,

$$\Phi(\tau, \tilde{k}) = \Phi_0(\tilde{k}) + \tau^{-1}\Phi_1(\tilde{k}) + O(\tau^{-2}) \quad (39)$$

one can write that

$$I(\tau) \underset{\tau \rightarrow \infty}{\approx} \text{saddle point expansion of } \int d\tilde{k} \exp[\tau\Phi_0(\tilde{k}) + \Phi_1(\tilde{k})] \quad (40)$$

In our case, the expansion (39) can be performed. The leading term, Φ_0 , is given by (cf. equation (34))

$$\Phi_0(\tilde{k}) = -i\tilde{k}\varepsilon + \frac{\gamma}{2} \left[1 + i\sqrt{4i\tilde{k} - 1} \right] \quad (41)$$

since as $\tilde{\gamma} \gg 1$, the x_n stack on \mathbb{R}^+ with a constant density $\tilde{\gamma}/\pi$ (cf. (29)) and sums can be replaced by integrals:

$$\sum_{n=0}^{\infty} \log \left[1 - \frac{4i\tilde{k}}{1+x_n^2} \right] \sim \frac{\tilde{\gamma}}{\pi} \int_0^{\infty} dx \log \left[1 - \frac{4i\tilde{k}}{1+x^2} \right] = -\tilde{\gamma} \left[1 + i\sqrt{4i\tilde{k} - 1} \right] \quad (42)$$

(note that $\sqrt{4i\tilde{k} - 1}$ is understood as a complex number with positive imaginary part ; this generates a cut located in $\tilde{k} \in [i] - \infty, -\frac{1}{4}]$).

As one must also compute Φ_1 , one will need also the τ^0 term of the previous expansion: let define $L(x) = \log(1 - 4i\tilde{k}/(1+x^2))$.

From (cf. eq. (29))

$$x_{n+1} - x_n = \pi/\tilde{\gamma} - \frac{2\pi}{\tilde{\gamma}^2} \frac{1}{1+x_n^2} + o(\tau^{-2}) \quad (43)$$

one has (we show some details because this expansion is delicate)

$$\begin{aligned}
& \sum_{n=1}^{\infty} L(x_n) - \frac{\tilde{\gamma}}{\pi} \int_0^{\infty} dx L(x) \\
&= \frac{\tilde{\gamma}}{\pi} \sum_{n=1}^{\infty} \int_{x_n}^{x_{n+1}} du \left[\frac{\pi}{\tilde{\gamma}(x_{n+1} - x_n)} L(x_n) - L(x) \right] - \frac{\tilde{\gamma}}{\pi} \int_0^{x_1} dx L(x) \\
&\sim \frac{\tilde{\gamma}}{\pi} \sum_{n=1}^{\infty} \int_{x_n}^{x_{n+1}} dx (L(x_n) - L(x)) + \frac{2}{\pi} \sum_n \int_{x_n}^{x_{n+1}} dx \frac{L(x_n)}{1+x_n^2} - \frac{\tilde{\gamma}}{\pi} \int_0^{x_1} dx L(x) \\
&\sim -\frac{\tilde{\gamma}}{2\pi} \sum_{n=1}^{\infty} (x_{n+1} - x_n)^2 L'(x_n) + \frac{2}{\pi} \int_0^{\infty} \frac{L(x)}{1+x^2} dx - \frac{\tilde{\gamma}}{\pi} \int_0^{x_1} L(x) \\
&\sim -\frac{1}{2} \int_{x_1}^{\infty} dx L'(x) + \frac{2}{\pi} \int_0^{\infty} \frac{L(x)}{1+x^2} dx - \frac{\tilde{\gamma}}{\pi} \int_0^{x_1} L(x)
\end{aligned} \tag{44}$$

One can ask why one keeps an explicit x_1 -dependence in the last expression, since up to order τ^0 , $\int_{x_1}^{\infty} dx L'(x) \sim -L(0)$ and $\tilde{\gamma}/\pi \int_0^{x_1} \sim L(0)$. The reason is that these expressions are not uniformly valid for any \tilde{k} , since $L(0) = \log(1 - 4i\tilde{k})$ diverges when $\tilde{k} \rightarrow -i/4$. Expression (44) is finally computed and (safely) approximated to

$$\begin{aligned}
& \sum_{n=1}^{\infty} L(x_n) - \frac{\tilde{\gamma}}{\pi} \int_0^{\infty} dx L(x) \approx -\frac{1}{2} \log \left(\frac{1 - 4i\tilde{k} + (\pi/\tilde{\gamma})^2}{1 + (\pi/\tilde{\gamma})^2} \right) \\
&+ 2 \log \frac{1 - i\sqrt{4i\tilde{k} - 1}}{2} + 2 \left(\frac{\tilde{\gamma}}{\pi} \text{Atan} \frac{\pi}{\tilde{\gamma}} - i \frac{\tilde{\gamma}}{\pi} \sqrt{4i\tilde{k} - 1} \text{Atan} \frac{\pi/\tilde{\gamma}}{i\sqrt{4i\tilde{k} - 1}} \right)
\end{aligned} \tag{45}$$

In (34), one has also to compute the second term, up to order τ^0 ; this is readily obtained since

$$\log \left(1 + 16\tilde{k}^2 \sum_{n=1}^{\infty} \frac{x_n^2}{1+x_n^2} \frac{1}{2 + \tilde{\gamma}(1+x_n^2)} \frac{1}{1 - 4i\tilde{k} + x_n^2} \right) \tag{46}$$

$$\sim \log \left[1 + \frac{16\tilde{k}^2}{\pi} \int_0^{\infty} dx \frac{x^2}{(1+x^2)^2} \frac{1}{1 - 4i\tilde{k} + x^2} \right] \tag{47}$$

$$= \log \left[1 - \frac{1}{4} \left(1 + i\sqrt{4i\tilde{k} - 1} \right)^2 \right] \tag{48}$$

This term is the cause of the other cut already mentioned (due to the presence of the \log), and is defined by $\tilde{k} \in]2, \infty[$. To summarize, one can notice that Φ_1 is $-1/2$ times the sum of (45) and (48).

The saddle point expansion can be performed on this integral by looking at paths where $\text{Im}(\Phi)$ remains zero. One sets $\sqrt{4i\tilde{k} - 1} = u + iv$ (with $v > 0$ compulsorily), and finds easily that these paths are characterized by $u = 0$ or $v = \gamma/\varepsilon$ (this term is allowed only if $\varepsilon > 0$). As $\tilde{k} = uv/2 + i(v^2 - u^2 - 1)/4$, one sees that these “real” paths are like on the figure 2. The saddle point method then tells us to perform the integration along the “real” path which makes $\text{Re}[\Phi]$ vanishing at ∞ (i.e. here the parabola). But this scheme can actually be perturbed by the presence of the upper cut (due to the term (48)): if $\varepsilon > \gamma/3$, the parabolic path does not meet any cut, and no complication occurs. On the contrary, if

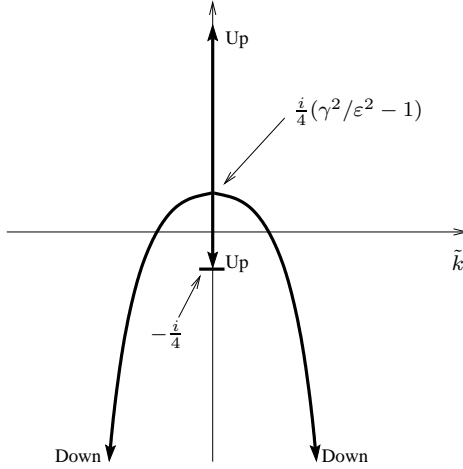


Figure 2: Paths where equation $\text{Im}[\Phi(\tilde{k})] = 0$ is verified for $\varepsilon \geq 0$. One indicates also the schematic behaviour of $\text{Re}[\Phi]$ along these paths : if it grows to ∞ or decreases to $-\infty$. The saddle is located at the crossing of the two paths. Note that the parabolic-shaped path does no longer exist on if $\varepsilon < 0$, but in that case the vertical path vanishes at infinity.

$\varepsilon \leq \gamma/3$, the parabola crosses the cut, and the path must consequently be modified to avoid such a crossing : it crawls along the cut from the crossing point to the end of the cut (at $\tilde{k} = 2i$), crawls back to the crossing point along the other side of the cut, and then meets the other branch of the parabola (cf. figure 3). Notice that the parabola disappears if $\varepsilon < 0$ and the path sticks completely along the upper cut (what is coherent with the convergence of the integral ...).

One can then perform the so-called Laplace method on these integrals, since the principal term in the exponential is purely real. It is worth noticing that the geometrical location of the saddle changes when ε crosses $\gamma/3$ (but this change remains continuous), what is quite surprising, since no special dynamical event occurs at this value. This leads to a curious result, with two different behaviours :

$$\pi_{\text{inj}}(\tilde{\varepsilon}) \sim \begin{cases} P_> \exp\left(-\frac{(\tilde{\varepsilon} - \tilde{\gamma})^2}{4\tilde{\varepsilon}}\right) & \text{if } \varepsilon > \gamma/3 \\ P_< \exp(2\tilde{\varepsilon} - \tilde{\gamma}) & \text{if } \varepsilon < \gamma/3 \end{cases} \quad (49)$$

with

$$P_> = \frac{2\tilde{\gamma}}{\sqrt{\pi\varepsilon^3}} \left(\frac{\tilde{\gamma}^2/\tilde{\varepsilon}^2 + \pi^2/\tilde{\gamma}^2}{1 + \pi^2/\tilde{\gamma}^2} \right)^{\frac{1}{4}} \frac{1}{\sqrt{(1 + \tilde{\gamma}/\tilde{\varepsilon})^3(3 - \tilde{\gamma}/\tilde{\varepsilon})}} \exp\left(-\frac{\tilde{\gamma}}{\pi} \left[\text{Atan}\frac{\pi}{\tilde{\gamma}} - \frac{\tilde{\gamma}}{\tilde{\varepsilon}} \text{Atan}\frac{\tilde{\varepsilon}\pi}{\tilde{\gamma}} \right] \right) \quad (50)$$

$$P_< = \frac{(3/2)^{3/2}}{\sqrt{\pi\tilde{\varepsilon}}} \frac{1}{\sqrt{\tilde{\gamma}/\tilde{\varepsilon} - 3}} \quad (51)$$

It is worth noticing that these prefactors have two different behaviours : $P_<$ decreases like $(-\tilde{\varepsilon})^{-1/2}$ for large $|\tilde{\varepsilon}|$, whereas $P_>$ behaves like $\tilde{\varepsilon}^{-3/2}$; however, for this latter case, one could observe for very large τ a region with a $\tilde{\varepsilon}^{-2}$ relaxation (actually when $\tilde{\varepsilon} \ll \tilde{\gamma}^2$).

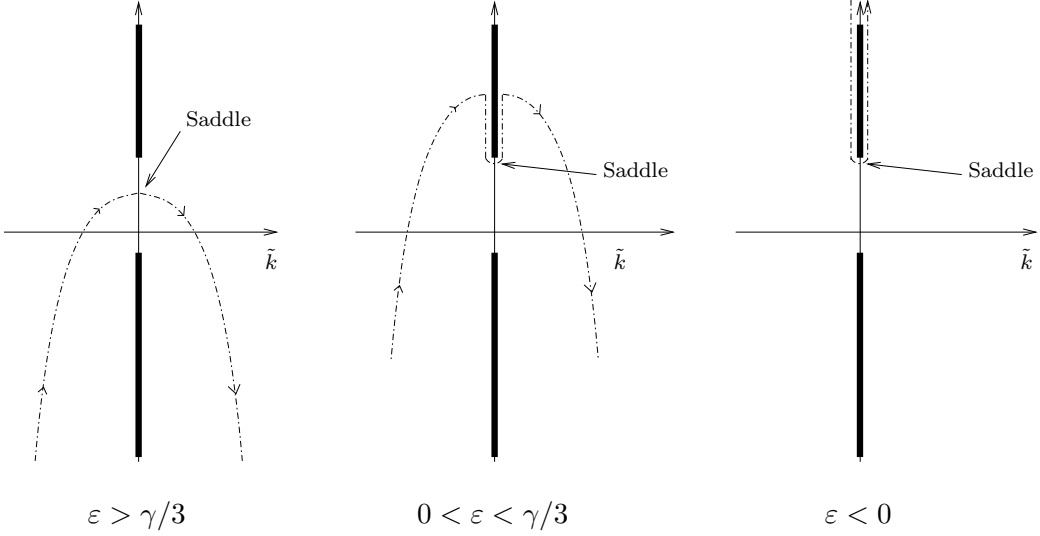


Figure 3: Sketch of different “real” paths, according to the values of ε/γ .

Prefactors $P_<$ and $P_>$ display an (integrable) divergence around $\gamma/3$, due to the collapse of the two saddles of figure 3 : actually, the saddle expansion of (49) is not valid within a window of size $1/\sqrt{\tau}$ around $\tilde{\gamma}/3$; a correct expansion at $\tilde{\varepsilon} = \tilde{\gamma}/3$ gives rather

$$\pi_{inj}(\tilde{\gamma}/3) \sim \frac{3^{3/2}}{2\pi} e^{-\tilde{\gamma}/3} \left(\frac{3}{\tilde{\gamma}}\right)^{1/4} \underbrace{\int_0^\infty dr e^{-r^4}}_{\approx 0.906} \quad (52)$$

To obtain corrected expressions, where this unphysical divergence is removed, one must perform the saddle point expansion of (40) a bit less abruptly. For this purpose, one evaluates Φ_1 at the saddle (i.e. $\tilde{k} = i(\tilde{\gamma}/\tilde{\varepsilon})^2/4$ if $\tilde{\varepsilon} > \tilde{\gamma}/3$, $\tilde{k} = 9i/4$ if $\tilde{\varepsilon} < \tilde{\gamma}/3$), except for the term responsible for the divergence $-\frac{1}{2} \log(1 - (1 + i\sqrt{4i\tilde{k} - 1})^2/4)$. The remaining integral is then deformed to stick along the negative cut if $\varepsilon > 0$ and along the positive cut if $\varepsilon < 0$: one abandons the saddle path, for it is now of no special importance, since one will keep entirely the remaining integral¹.

One gets more involved expressions which can be easily evaluated with numerical integration : let define

$$v_c = \begin{cases} \tilde{\gamma}/\tilde{\varepsilon} & \text{if } \tilde{\varepsilon} > \tilde{\gamma}/3 \\ 3 & \text{if } \tilde{\varepsilon} < \tilde{\gamma}/3 \end{cases} \quad (53)$$

$$\chi(\tilde{\varepsilon}) = \left(\frac{v_c^2 + \pi^2/\tilde{\gamma}^2}{1 + \pi^2/\tilde{\gamma}^2} \right)^{\frac{1}{4}} \frac{2}{1 + v_c} \exp \left(-\frac{\tilde{\gamma}}{\pi} \left[\text{Atan} \frac{\pi}{\tilde{\gamma}} - v_c \text{Atan} \frac{\pi}{v_c \tilde{\gamma}} \right] \right) \quad (54)$$

¹finding the saddle path is nevertheless unavoidable to determine the precise location of the saddle point used for the evaluation of the approximated part of Φ_1

We have the result

$$\pi_{inj}(\tilde{\varepsilon}) = \begin{cases} \chi(\tilde{\varepsilon}) \times \left(-\frac{\partial}{\partial \tilde{\gamma}} + \frac{1}{2} \right) \int_{-\infty}^{\infty} \frac{d\theta}{\pi} \exp \left(-\tilde{\varepsilon} \sinh^2 \theta - \frac{(\tilde{\gamma} - \tilde{\varepsilon})^2}{4\tilde{\varepsilon} \cosh^2 \theta} \right) & \text{if } \tilde{\varepsilon} \geq 0 \\ \chi(\tilde{\varepsilon}) \times \left(-\frac{\partial}{\partial \tilde{\gamma}} + \frac{1}{2} \right) \int_{-\infty}^{\infty} \frac{d\theta}{\pi} \exp \left(\tilde{\varepsilon} \cosh^2 \theta + (\tilde{\varepsilon} - \tilde{\gamma}) \cosh \theta \right) & \text{if } \tilde{\varepsilon} \leq 0 \end{cases} \quad (55)$$

2.8 Discussion

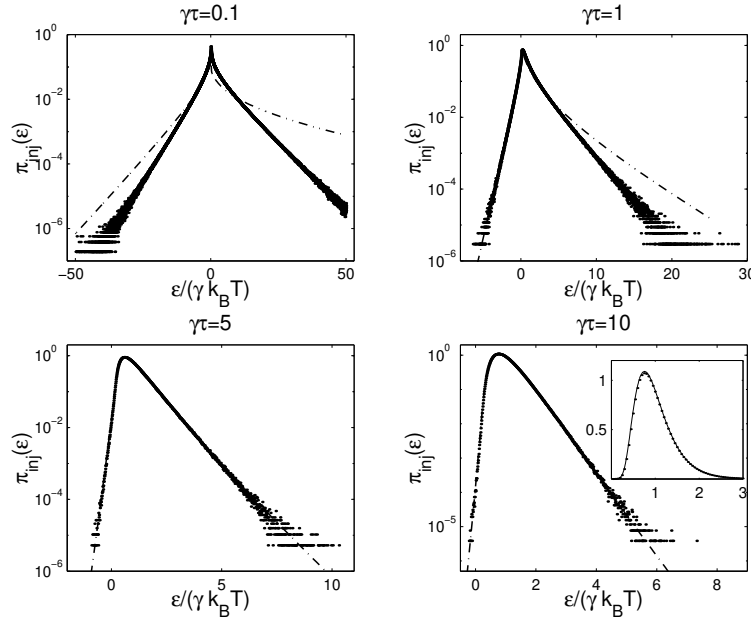


Figure 4: Semilog plots of the pdf of injected power $\pi_{inj}(\varepsilon)$ for several values of $\tilde{\gamma} = \gamma\tau$. One plots together the formula (55) (dashed line) and results of numerical simulations (dots), which are almost superimposed for $\gamma\tau = 5$ and $\gamma\tau = 10$. The insert in the last plot is the corresponding linear version.

This result is plotted on fig. 4 for different values of $\tilde{\gamma}$, together with numerical simulations: it shows that this limiting formula is a very good approximation of the true pdf even if $\tilde{\gamma} \approx 5$. These pdf are rather asymmetric with respect to their maximum, even in the limit of large τ : the right tail of the pdf falls off as $\frac{1}{\varepsilon^{3/2}} \exp(-\varepsilon\tau/4k_B T)$, whereas the left tail vanishes more rapidly, as $\frac{1}{\varepsilon^{1/2}} \exp(2\varepsilon\tau/k_B T)$. This is at first sight surprising, because as the renewal of the noise ψ is independent of the particle velocity v , occurrences of positive or negative instantaneous power injection ψv are completely equiprobable. Actually, the long time interval during which the mean is performed is of crucial importance and is responsible for the peculiar shape of the pdf; to understand this, let us consider an occurrence of a (rare) large positive fluctuation of injected power: this occurrence understands that a favourable sampling of the noise is realized, so that very often the noise gives energy to the particle. Consequently, during the process, the energy has a global tendency to increase, as well as typical values of the velocity; as the injected power is directly proportional to the velocity, one sees that the direct effect of the positive injection of energy is to enhance typical values

of v implied in the evaluation of ε : this favourable feedback makes finally the occurrence of the considered fluctuation more likely, since less efficiency of the noise is globally required to generate the fluctuation.

On the contrary, let us consider a (large) negative fluctuation: the scenario is here inverted, since the typical velocity will certainly decrease during the mean process: to ensure the large expected value of power ceded back to the bath, one is then compelled to begin the motion with a large kinetic energy, what is exponentially unprobable: the feedback is here clearly unfavourable, and diminishes comparatively the frequency of such occurrences. To highlight this duality, one can compute the “optimal fluctuation”, that is, the extrema of ε which can occur for a fixed value of $C = \gamma \int_{-\tau/2}^{\tau/2} \psi^2$, given the initial velocity of the particle. The result (see Appendix A for details),

$$2\tau\varepsilon_{opt}^\pm = C \pm \sqrt{(C + v_0^2)^2 - v_0^4} \quad (56)$$

confirms the preceding discussion: there is typically two situations which make large positive fluctuation of ε possible: sampling a large initial value of v_0 , or a noise with large $\int \psi^2$ will both ensure a large occurrence of ε . On the contrary, there is only one way to realize a large negative fluctuation (large value of v_0): for small initial velocities, optimal fluctuation ε_{opt}^- goes to zero like v_0^2 , displaying explicitly the origin of the asymmetry of π_{inj} . Furthermore, this is confirmed by the remarks made throughout the calculation, when one noticed that the negative fluctuations were strongly associated with the past of the particle: this past is indeed of great importance to allow the particle to generate an extreme value of v_0 , its velocity at the beginning of the mean window.

2.9 Test of Fluctuation theorem

Our model is a good system to test the possible universality of the (Evans-Cohen-Morris) fluctuation theorem, since the exact result is at hand. From (49), one has

$$\rho(\varepsilon) \equiv \frac{1}{\tau} \log \frac{\pi_{inj}(\varepsilon)}{\pi_{inj}(-\varepsilon)} \underset{\tau \rightarrow \infty}{\sim} \begin{cases} \frac{4}{k_B T} \frac{\varepsilon}{\gamma} & \text{if } \varepsilon < \gamma/3 \\ \frac{7}{4} \frac{\varepsilon}{k_B T} + \frac{3}{2} \gamma - \frac{\gamma^2}{4\varepsilon/k_B T} & \text{if } \varepsilon > \gamma/3 \end{cases} \quad (57)$$

This function is clearly not a straight line, in disagreement with the fluctuation theorem: we exhibit here an example where this theorem is not fulfilled. On this negative result can we make two comments: first, it is not contradictory with those of Kurchan [8]. One looks for the power injected by the fluctuation in a system where a fluctuation/dissipation balance exists, whereas the fluctuation theorem established by Kurchan considers the power injected by an *external* operator in a system in equilibrium with a thermostat. We already noticed that the first situation is much more appropriate to describe realistic systems driven far from equilibrium. Second, formula (57) illustrates well the fact that fluctuation theorem seems to hold in so large a number of experimental situations, as explained in [4]: in the vicinity of $\varepsilon = 0$, $\rho(\varepsilon)$ must always have a straight line behaviour, as a consequence of the large deviation law; on the other hand, as large negative values of ε are extremely unprobable when τ is large, it becomes practically unpossible even to only measure $\rho(\varepsilon)$ for large ε and large τ with enough statistical resolution: possible deviations from the straight line are just even not measurable. In our case, crossover occurs for $\varepsilon = \gamma/3$ and for this value, $\pi_{inj} \propto \exp(-5\gamma\tau/3)$ which is of order 10^{-8} only if $\gamma\tau = 10 \dots$ Our model is thus a good illustration in favour of arguments given in [4] against the full generality of the fluctuation theorem.

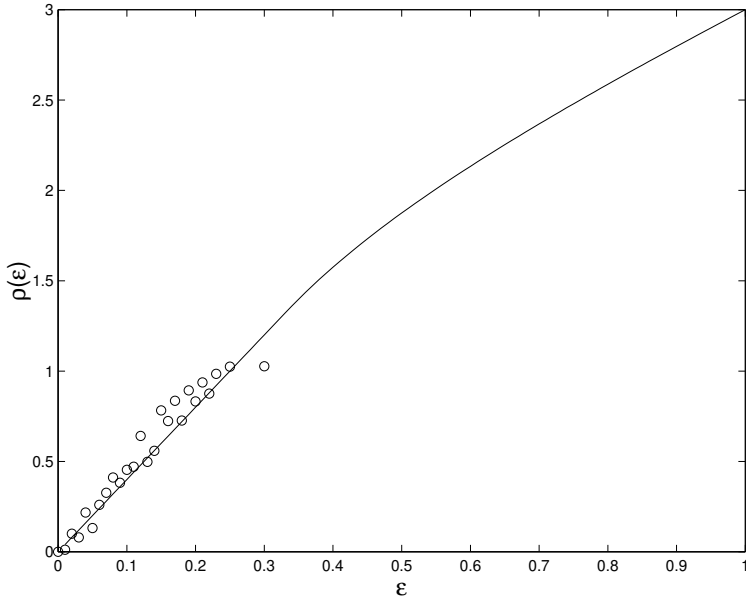


Figure 5: Function $\tau^{-1} \log[\pi_{inj}(\varepsilon)/\pi_{inj}(-\varepsilon)]$ for $\gamma = 1, \tau = 8$. Circles come from numerics with two millions points of statistics, and stop before the crossover of the theoretical curve (solid) due to the lack of negative points with large absolute value.

2.10 Beyond the free Brownian motion

The reasoning concerning the asymmetry of π_{inj} suggests that certain characteristics of this pdf seem—in the limit of large τ only—to be independent of the details of the particle dynamics, since it is based only on considerations on energy and its conservative character. These observations led us to infer a possible insensitivity of π_{inj} with respect to other microscopic times than γ^{-1} (γ^{-1} itself cannot be neglected, since this time plays a role in the process of dissipation of energy; and indeed, the curves for different γ have different and non superposable shapes), in cases where the initial system would have been complexified. Thus, we considered several confined Langevin systems:

$$\ddot{x} + \gamma \dot{x} + V'(x) = \psi(t) \quad (58)$$

$$\langle \psi(t)\psi(t') \rangle = 2\gamma k_B T \delta(t - t') \quad (59)$$

where we used for $V(x)$ an harmonic potential $V(x) = \frac{1}{2}\omega^2 x^2$, a non linear “hard” potential $V(x) = \frac{1}{2}\omega^2 x^2 + \frac{\alpha}{4}x^4$ ($\alpha > 0$), a non linear asymmetric “soft” potential $V(x) = \omega^2(\alpha^2 e^{-x/\alpha} + \alpha x)$, and also a bistable φ^4 potential $V(x) = V_b(x^2 - 1)^2$. We numerically calculated for all these potentials (as well as again the free case for comparison) the pdf π_{inj} , for large values of τ ($\gamma = 1$ for convenience).

The results (see fig. 6) are extraordinarily surprising, since one cannot distinguish the different curves from each other! One must keep in mind the fact that the dynamical behaviour of $x(t)$ is completely different in all these cases: fully isochronic or anisochronic oscillatory, overdamped, bistable, diffusive, these different Brownian motions lead all to apparently the *same* curve, a coincidence which goes beyond all expectations and put down interesting questions: why a so close correspondence between these models? Is this kind of “universality”

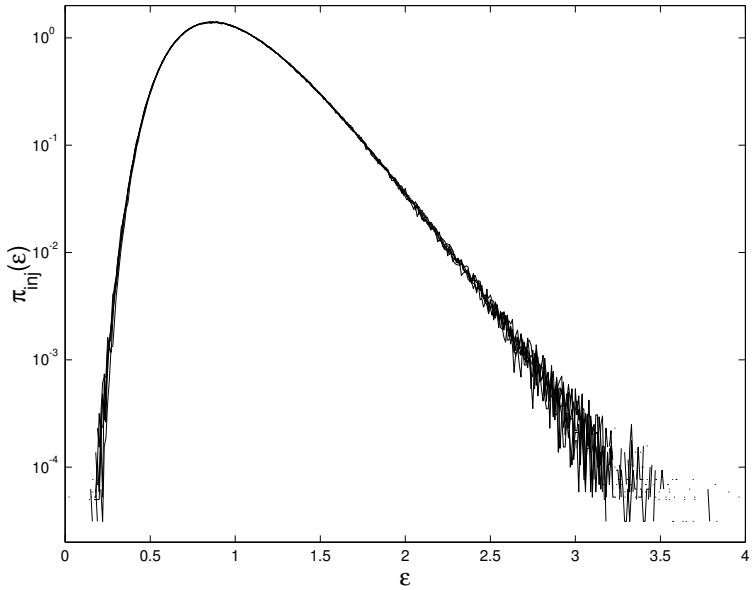


Figure 6: Injected power pdf for several trapped Langevin particles with $k_B T = 1$, $\tau = 20$ and $\gamma = 1$: three harmonic potentials (free motion $\omega = 0$, $\omega = 1$ and $\omega = 10$), hard and soft nonlinear potentials ($\omega = 1, \alpha = 3$ in both cases), bistable φ^4 -potential with $V_b = 1$ (strong anharmonicity is explored in this case – see details in text).

a consequence of the fluctuation/dissipation balance, or as expected and wished an evidence for common features of the energy flow which transcend dynamical peculiarities ? In that case, can we use this study of Brownian motion to characterize realistic dissipative systems where the injection of energy is usually restricted to the boundaries of the system ? Finally, is it possible to give sense by means of π_{inj} to a concept of out-of-equilibrium temperature? By examining the intimate details of the computation, it appears that π_{inj} could provide interesting generalizations, for instance to situations displaying aging, for in that case the left tail of the distribution would be certainly deeply affected by the unpossibility for the system to reach equilibrium distribution at the beginning of the averaging window.

3 Conclusion

In this paper, we exposed the computation of the pdf of power injected by the random force into a Brownian particle described by a Langevin equation. The formal result is quite complicated, but the long-time average limit gives much more simple results, which match very accurately the numerical simulations. We discussed also some physical properties of the pdf, namely the very origin of its asymmetry, and this discussion led us to compute numerically the same pdf for more involved Langevin dynamics. These simulations gave very surprising results, because for fixed values of γ and τ , all different models led at first sight to the *same* pdf in the limit $\gamma\tau \gg 1$, despite the great variety of type of individual particle motions.

This adequation is still largely to be understand, and this part of the work is presently

in progress. The first task we are now working on is to compute the case of harmonically bounded Langevin particle, for the above presented calculation can *a priori* be adapted for this linear model. This computation could demonstrate rigorously the merging of its pdf with the free case in the large τ limit, and gives some clues toward a better understanding of this phenomena. Concerning non linear models, a renormalization scheme could then from this certainly be constructed.

4 Acknowledgments

I am much indebted to S.Fauve, R.Labbé, S.Aumaître, F.Pétrelis, R.Berthet, N.Mujica, R.Wunenburger and B.Derrida for fruitful discussions.

Appendix A: Optimal fluctuations

We want to compute the optimal positive ε_+ or negative ε_- fluctuation of averaged injected power, knowing the initial (i.e. at time $-\tau/2$) value of the velocity v_0 , and under the constraint $\int_{-\tau/2}^{\tau/2} \psi^2 = \gamma C$.

Since

$$v(t) = v_0 \exp(-\gamma[t + \tau/2]) + \int_{-\tau/2}^t du e^{-\gamma(t-u)} \psi(u), \quad (60)$$

one can write the “action” to be extremalized as

$$S[\psi] = \frac{1}{\tau} \int_{-\tau/2}^{\tau/2} dt \psi(t) \left[v_0 e^{-\gamma(t+\tau/2)} + \int_{-\tau/2}^t du e^{-\gamma(t-u)} \psi(u) \right] + \frac{\lambda}{\gamma \tau} \int_{-\tau/2}^{\tau/2} \psi^2 \quad (61)$$

$$= \frac{1}{2\tau} \int \psi \mathcal{T} \psi + \frac{v_0}{\tau} (\mathcal{T} \psi)_{(-\tau/2)} + \frac{\lambda}{\gamma \tau} \int \psi^2 \quad (62)$$

where λ is (up to a factor $1/\gamma \tau$) the Lagrange multiplier associated with the constraint. Optimal fluctuations are thus solutions of

$$\mathcal{T} \psi + 2 \frac{\lambda}{\gamma} \psi + v_0 e^{-\gamma(t+\tau/2)} = 0 \quad (63)$$

To proceed farther, one is led to write ψ and $F = v_0 e^{-\gamma(t+\tau/2)}$ as $\psi = \psi_{\parallel} + \psi_{\perp}$ and $F = F_{\parallel} + F_{\perp}$, where X_{\parallel} is the orthogonal projection of X onto the subspace $\text{Im} \mathcal{T}$. One then expands ψ_{\parallel} over the ϕ_n (eigenfunctions of \mathcal{T}), i.e. $\psi_{\parallel} = \sum a_n \phi_n$, and (63) is equivalent to

$$F_{\perp} + 2 \frac{\lambda}{\gamma} \psi_{\perp} = 0 \quad \text{and} \quad (64)$$

$$\mathcal{T} \psi_{\parallel} + F_{\parallel} + 2 \frac{\lambda}{\gamma} \psi_{\parallel} = 0 \iff a_n = -\frac{v_0 \xi_n \phi_n(-\tau/2)}{\xi_n + 2\lambda/\gamma} \quad (65)$$

The value of λ is determined by the constraint:

$$\gamma C = \int \psi^2 = \sum_n a_n^2 + \int \psi_{\perp}^2 \quad (66)$$

$$= \sum_n a_n^2 + \frac{\gamma^2}{4\lambda^2} \left[\int F^2 - v_0^2 \sum \xi_n^2 \phi_n^2(-\tau/2) \right] \quad (67)$$

In the limit of large τ , one can simplify this last expression, as well as those corresponding to the value of the fluctuation (it is worth noting that the orthogonal part of the expansion becomes exponentially negligible when τ is increased):

$$\frac{C}{v_0^2} = \frac{(\sqrt{1 + \lambda^{-1}} - 1)^2}{2\sqrt{1 + \lambda^{-1}}} \quad (68)$$

$$\varepsilon_{opt} = \frac{v_0^2}{2\tau} \left(\frac{1}{\sqrt{1 + \lambda^{-1}}} - 1 \right) \quad (69)$$

Finally, when λ is expressed by means of C , one has the two (positive and negative) optimal fluctuations

$$\varepsilon_{opt}^{\pm} = \frac{C}{2\tau} \left(1 \pm \sqrt{1 + \frac{2v_0^2}{C}} \right) \quad (70)$$

Appendix B: Fluctuations of the dissipated power

The pdf of the dissipated power

$$\delta = \frac{1}{\tau} \int_t^{t+\tau} dt' \gamma v^2(t') \quad (71)$$

can be computed along the same line of calculus as before. We give here a slightly different way to handle the problem, solving first for a dissipation *knowing the initial velocity v_0 of the particle*, and averaging then over v_0 , an average who plays the role of the past history of the particle which ensured the thermalisation in the preceding situation.

According to this, one can write (the origin of the average window is placed at $t = -\tau/2$ for sake of coherence with preceding developments)

$$\langle e^{ik\delta} \rangle = \int \frac{dv_0}{\sqrt{2\pi k_B T}} e^{-\frac{1}{2} \frac{v_0^2}{k_B T}} \int \mathcal{D}\psi e^{-\frac{1}{4\gamma k_B T} \int_{-\tau/2}^{\tau/2} \psi^2} \times \exp \left[ik \frac{\gamma}{\tau} \int_{-\tau/2}^{\tau/2} dt \left(v_0 e^{-\gamma(t+\tau/2)} + \int_{-\tau/2}^t du e^{-\gamma(t-u)} \psi(u) \right)^2 \right] \quad (72)$$

In the limit of large τ , one has, up to a negligible factor proportional to $e^{-2\gamma\tau}$,

$$\langle e^{ik\delta} \rangle = \int \frac{dv_0}{\sqrt{2\pi k_B T}} e^{-\frac{1}{2} \frac{v_0^2}{k_B T}} \int \mathcal{D}\psi e^{-\frac{1}{4\gamma k_B T} \int \psi^2} \exp \left[\frac{ik}{2\tau} \left(v_0^2 + 2v_0 (\mathcal{T}\psi)_{(-\tau/2)} + \int \psi \mathcal{T}\psi \right) \right] \quad (73)$$

For Gaussian integrals, one knows that the saddle point expansion is exact; thus,

$$\langle e^{ik\delta} \rangle = \int \frac{dv_0}{\sqrt{2\pi k_B T}} e^{-\frac{1}{2} \frac{v_0^2}{k_B T}} \exp \left[-\frac{1}{4\gamma k_B T} \int \psi_s^2 + \frac{ik}{2\tau} \left(v_0^2 + 2v_0 (\mathcal{T}\psi_s)_{(-\tau/2)} + \int \psi_s \mathcal{T}\psi_s \right) \right] \times \int \mathcal{D}\zeta e^{-\frac{1}{4\gamma k_B T} \int \zeta^2} \exp \left[\frac{ik}{2\tau} \int \zeta \mathcal{T}\zeta \right] \quad (74)$$

where ψ_s is the saddle path, solution of

$$-\frac{1}{2\gamma k_B T} \psi_s + \frac{ikv_0}{\tau} e^{-\gamma(t+\tau/2)} + \frac{ik}{\tau} \mathcal{T}\psi_s = 0 \quad (75)$$

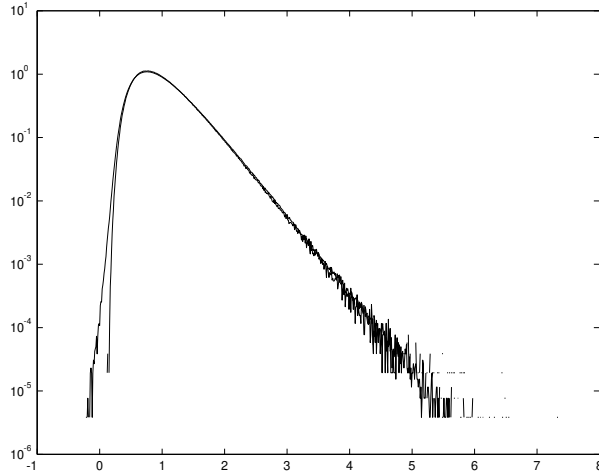


Figure 7: Injected and dissipated power pdf for the free Brownian motion ($\gamma = 1, k_B T = 1, \tau = 10$). The two distributions are very similar but in the vicinity of zero, partly due to the constraint $\gamma v^2 \geq 0$, whereas $\psi v \leq 0$.

This saddle path is easily computed using the appendix A, and one obtains (one recalls that $\tilde{k} = k \times k_B T / \tau$)

$$\langle e^{ik\delta} \rangle = \int \frac{dv_0}{\sqrt{2\pi k_B T}} \exp \left[-\frac{1}{2} \frac{v_0^2}{k_B T} + \frac{ikv_0^2}{2\tau} - \frac{ikv_0^2}{2\tau} \frac{\sqrt{1-4i\tilde{k}}-1}{\sqrt{1-4i\tilde{k}}+1} \right] \times \int \mathcal{D}\zeta e^{-\frac{1}{4\gamma k_B T} \int \zeta^2} \exp \left[\frac{ik}{2\tau} \int \zeta \mathcal{T} \zeta \right] \quad (76)$$

$$= \exp \left(-\frac{1}{2} \sum_{n=1}^{\infty} \log \left(1 - \frac{4i\tilde{k}}{1+x_n^2} \right) - \frac{1}{2} \log \left(1 - \frac{2i\tilde{k}}{\sqrt{1-4i\tilde{k}}+1} \right) \right) \quad (77)$$

From this formula, an inversion procedure similar to those explained for the injected power can be performed in the large τ limit. A fundamental discrepancy exists nevertheless with respect to the injected power, due to the fact that the second logarithm in (77) does not induce a positive vertical cut in the \tilde{k} space: this reflects the obvious fact that negative fluctuations of γv^2 never occur. As a result, it is easy to see that the large deviations function for the dissipated power is given by

$$f(\delta) = \frac{1}{\tau} \log \pi_{diss}(\delta) \underset{\tau \rightarrow \infty}{=} \begin{cases} -\frac{(\delta/k_B T - \gamma)^2}{4\delta/k_B T} & \text{if } \delta > 0 \\ 0 & \text{if } \delta \leq 0 \end{cases} \quad (78)$$

Thus, the large deviations functions of injected and dissipated power are exactly the same in the range $[\gamma/3, \infty[$, discrepancies arising only below this odd value $\gamma/3$. Consequently, one expects a certain similarity between the two distributions in their right tail to exist, a difference being possibly still observable in the left one: figure 4 illustrates this similarity. Of course, refinements similar to (55) are also possible, but the shape of the pdf is mainly governed by the exponential term $\exp(\tau f(\delta))$.

References

- [1] R.Labbé, J.F.Pinton, S.Fauve, *J.Phys. II France*, **6** (1996) 1099.
- [2] S.Aumaître, S.Fauve, *J. Chim. Phys.*, **96** (1999), 1038.
- [3] S.Aumaître, S.Fauve, J.F.Pinton, *Eur. Phys. J. B.*, **16** (2000), 563.
- [4] S.Aumaître, S.Fauve, S.McNamara, P.Poggi, *Eur. Phys. J. B.*, **19** (2001), 449.
- [5] D.J.Evans, E.G.D. Cohen, G.P.Morris, *Phys. Rev. Lett.*, **71** (1993), 2041.
- [6] G.Gallavotti, E.G.D. Cohen, *Phys. Rev. Lett.*, **74** (1995), 2694.
- [7] Courant & Hilbert, *Methods of Mathematical Physics I*, Wiley 1989.
- [8] J.Kurchan, *J.Phys. A*,**31** (1998), 3719.